Journal of
Applied Research in Water and Wastewater
Journal homepage: www.arww.razi.ac.ir

Original paper

Degradation of Enrofloxacin antibiotic in contaminated water by ZnO/Fe_2O_3/Zeolite nanophotocatalyst

Simin Shokrolahi, Mehrdad Farhadian*, Nila Davari

Department of Chemical Engineering, Faculty of Engineering, University of Isfahan, Isfahan, Iran.

GRAPHICAL ABSTRACT

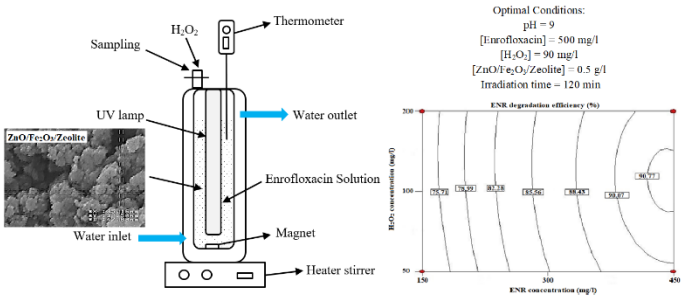

ARTICLE INFO

Article history:
Received 26 October 2019
Received in revised form 2 December 2019
Accepted 4 December 2019

Keywords:
Enrofloxacin
Antibiotic
Nanophotocatalyst
Water treatment
Environment

ABSTRACT

ZnO/Fe_2O_3/Zeolite nanophotocatalyst was synthesized by sol-gel method, and its performance in degradation of ENR, as one of the most commonly used veterinary antibiotics, is evaluated. The synthesized nanophotocatalyst is characterized by XRD, XRF, FT-IR, FE-SEM, EDX, and BET analyses. According to XRD, FT-IR, and EDX, presence of ZnO and Fe_2O_3 on the zeolite surface is confirmed. Based on XRF results, the optimal molar value of Fe^{3+}/ZnO in the synthesized nanophotocatalyst is obtained as 0.06. The FE-SEM results confirm the deposition of ZnO/Fe_2O_3 on the zeolite surface and indicate the approximate size of the photocatalyst particles as 48 nm. According to BET results, the specific surface area and pore volume for the synthesized nanophotocatalyst are obtained as 280.16 m^2/g and 0.35 cm^3/g, respectively. The simultaneous effects of operational factors, including the concentration of pollutant (150-450 mg/l), initial pH of the solution (5-9), and H_2O_2 concentration (50-200 mg/L) are examined on the ENR degradation efficiency via RSM. The results demonstrate that ENR concentration, pH, and H_2O_2 concentration have significant impacts on the ENR degradation efficiency in turn. According to the experimental results under optimal conditions (pH, contaminant concentration, and H_2O_2 concentration: 9, 500 mg/l, and 90 mg/l, respectively), the ENR degradation efficiency is 97.4%. This study suggests that the synthesized nanophotocatalyst has an acceptable efficiency to degrade a non-biodegradable contaminant.

1. Introduction

In recent decades, pharmaceutical compounds have been identified as an environmental issue, so the presence of antibiotics in environment seriously threaten the health of living creatures (Yi et al. 2019). ENR is a FQ which is used in veterinary medicine for treating breathing diseases, skin infections, and bacterial infections of animals (Anirudhan et al. 2017). Owing to extensive ENR consumption in animal husbandry and aquaculture, this animal antibiotic has a direct access to soil and groundwater through wastewater sludge or recycling of agricultural fertilizer from animal husbandry (Sturini et al. 2015). ENR has been recognized in surface water (4.4 ng/L), urban wastewater (0.7-8.3 ng/l), urban waters (2.8-8.3 ng/L), and sediments (123 ng/g) (Xiong et al. 2017). ENR has a mutagenic potential and drug resistance (Alexandrino et al. 2017). The presence of ENR in water even at very low concentrations damages the health of humans and marine creatures (Deng et al. 2018). Therefore, ENR removal from wastewater and water resources is vital considering its non-biodegradability, mutagenicity, and drug resistance (Wen et al. 2018). Researchers have utilized AOPs, including ozonolysis, sonolysis, UV/H_2O_2, photolysis, Fenton, photoelectron-Fenton, oxidation electrochemical, persulfate oxidation, and photocatalysis (Guo et al. 2017; Wang et al. 2017). The basis of these processes is to produce $^{\bullet}OH$, whereby the medicines are converted to CO_2, H_2O, and inorganic acids (Qiu et al. 2019). Photocatalytic processes are the most common AOPs widely used in the treatment of pharmaceutical effluents thanks to their high efficiency, production of non-toxic compounds, chemical stability, and reaction at room temperature (Yu et al. 2017). The removal of ENR has been

*Corresponding author Email: m.farhadian@eng.ui.ac.ir

examined through the following photocatalysts: TiO_2 (Anirudhan et al. 2017; Lu et al. 2014; Su et al. 2017; Yu et al. 2017), Graphene-like $BN/BiPO_4$ (Chen et al. 2017), Ag_2O/CeO_2 (Wen et al. 2018), Co_3O_4-composite (Deng et al. 2018), Fe_3O_4/MMT (Peng et al. 2019), and CuO (Fink et al. 2012). ZnO photocatalyst has a great characteristic in degrading non-biodegradable pollutants due to its high stability, recoverability, high photo sensitivity, and non-toxic nature (Amornpitoksuk et al. 2018; Nava Núñez and Martínez-de la Cruz. 2018). Therefore, ZnO has been commonly used in photocatalytic processes (Zhu et al. 2018). Furthermore, Fe_2O_3 is an effective factor in enhancing the photocatalytic properties of ZnO (Davari et al. 2019). Natural zeolites (clinoptilolite) have been used as the support of photocatalysts because of their high chemical stability, porous surface, large pore volume, and relative abundance in Iran (Arimi et al. 2016; Esmaili et al. 2017). Hybrid photocatalysts have greater photocatalytic activity, leading to higher degradation efficiency (Siwińska-Stefańska et al. 2018). To the best of our knowledge, this is the first study to investigate ENR degradation in polluted water with hybrid nanophotocatalyst consisting of ZnO and Fe_2O_3 supported on zeolite. In this study, by depositing ZnO/Fe_2O_3 on zeolite, a nanophotocatalyst is synthesized with a high efficiency in ENR degradation through sol-gel method. Following characterization, the synthesized nanophotocatalyst is used in an advanced oxidation reactor in order to degrade the contaminant. The effects of operational factors, including the antibiotic concentration, H_2O_2 concentration, and initial pH of the solution are investigated on the ENR degradation efficiency by RSM. Furthermore, the recoverability of the synthesized ZnO/Fe_2O_3/Zeolite nanophotocatalyst is evaluated in the ENR degradation.

2. Materials and methods

2.1. Chemicals

All chemicals used in this study are purchased from Merck. To synthesize ZnO/Fe_2O_3/Zeolite nanophotocatalyst, chemicals, namely $FeCl_3$ and $Zn(CH_3COO)_2{\cdot}2H_2O$ are utilized. To adjust pH of the solution, H_2SO_4 (purity 97 %), NaOH, and NH_4OH (purity 98 %) are used, respectively. In all of the experiments, H_2O_2 is applied as an oxidizing agent. Additionally, natural zeolite is obtained from mines of Semnan, Iran. Enrofloxacin (ENR) (purity around 98 %) attained from Sians Co., Iran. Physical and chemical properties of ENR are presented in Table 1.

Table 1. Specifications of ENR antibiotic (Dolar et al. 2013).

Pharmaceutical name	Enrofloxacin
Pharmaceutical type	Antibiotics
Molecular formula	$C_{19}H_{22}F_1N_3O_3$
Pharmaceutical structure	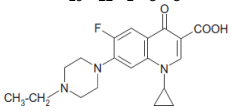
Molecular weight, g/mol	359.40
Solubility, mg/L	3397
λ_{max}, nm	275

2.2. Method for synthesis of ZnO/Fe_2O_3/Zeolite nanophotocatalyst

In order to synthesize ZnO/Fe_2O_3/Zeolite nanophotocatalyst via sol-gel method, the zeolite sample is prepared. It is then washed with deionized water and dried at room temperature. For achieving the maximum degradation efficiency based on screening tests, the optimal molar ratio of Fe^{3+}/ZnO as 0.06 is considered. Moreover, 1.35 g $Zn(CH_3COO)_2{\cdot}2H_2O$ and 0.06 g $FeCl_3$ are dissolved in 100 ml deionized water, after which the solution undergo ultrasound at 25 °C. Next, 0.47 g zeolite is added to the solution, and the pH is adjusted at around 7 by NH_4OH. The solution is stirred at 25 °C for 4 h and is left in the laboratory for 24 h to complete the reactions and form the gel. The solution is dried at 80 °C and 5 h in an oven, and the calcination process is performed in a muffled furnace at 350°C for 3 h to obtain ZnO/Fe_2O_3/Zeolite nanophotocatalyst (Davari et al. 2017).

2.3. Characterization of ZnO/Fe_2O_3/Zeolite nanophotocatalyst

Various analyses are utilized for characterization of zeolite and ZnO/Fe_2O_3/Zeolite nanophotocatalyst. XRF analysis is used to determine the composition of different elements in the structure of zeolite and the synthesized nanophotocatalyst. XRF analysis is conducted by an X-ray fluorescence device (S4-Pioneer, Bruker, Germany). FT-IR analysis is also performed to determine the functional groups by a Fourier transform infrared spectrometer device (FT-IR-6300, Jasco, Japan). BET analysis is conducted with the aim of investigating specific surface area and pore volume of zeolite and the synthesized nanophotocatalyst by means of N_2 adsorption at 77 K (Belsorp mini, Japan). FE-SEM images are obtained by a FE-SEM device (S-4160, Hitachi, Japan). The morphology and structure of zeolite as well as the synthesized nanophotocatalyst are examined by a scanning electron microscopy device (SEM, XL series, Phillips XL30) equipped with EDX analysis (AIS2300C, SERON technology). XRD analysis is used for identifying ZnO and Fe_2O_3 on zeolite and confirming stability of zeolite after deposition of nanoparticles on it. XRD analysis is performed by an X-ray diffraction device (D-8 Advance, Bruker, Germany).

2.4. Experimental photoreactor

In this study, a double-walled glass reactor with an approximate volume of 250 ml is used, in which a UV lamp (8 W, 254 nm) is located. The reactor temperature is adjusted at 25±1°C through water circulation in cooling pipes devised around the reactor. The solution homogeneity is considered by a magnetic stirrer and magnet. The utilized experimental system is demonstrated in Fig. 1.

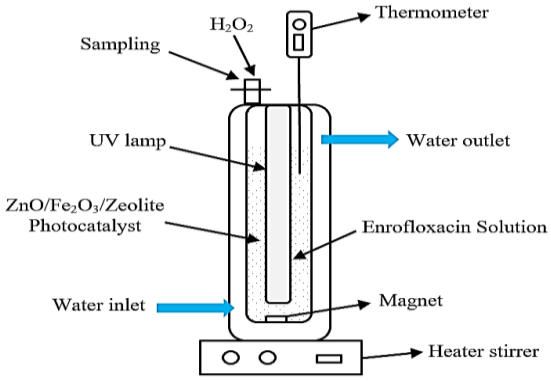

Fig. 1. Experimental system.

2.5. Design of experiments

In this study, response surface methodology (RSM) is utilized for the photocatalytic degradation of ENR. According to Table 2, operational factors, including ENR concentration, H_2O_2 concentration, and initial pH of the solution are examined, and other factors such as temperature (25±1 °C) as well as the intensity of UV lamp radiation (8 W power, 254 nm wavelength) are assumed constant. Based on the screening experiments, optimal values for ZnO/Fe_2O_3/Zeolite nanophotocatalyst within the range of 0.25-1 g/L and the irradiation time of 45-180 min are considered as 0.5 g/l and 120 min, respectively.

Table 2. Selected factors and levels in the photocatalytic degradation of ENR.

Factors	Levels		
Enrofloxacin concentration, mg/L	150	300	450
H_2O_2 concentration, mg/L	50	100	200
Initial pH	5	7	9

2.6. Procedure of ENR photocatalytic experiments

For each experiment, a solution of ENR with the desired concentration is prepared and its pH is adjusted by diluted solutions of H_2SO_4 and using a pH meter (UB-10, Denver Co.). Moreover, in each experiment, the concentration of ZnO/Fe_2O_3/Zeolite nanophotocatalyst (0.5 g/L) is added to the photoreactor with certain amounts of H_2O_2. In order to separate the photocatalyst particles in the solution, a centrifuge device (UniCen, Herolab Model, Herolab Co., Germany) is used within 10 min at 5000 rpm. The output concentration of ENR is determined by a spectrophotometer device (V-570, Jasco, Japan) using the calibration curve at its maximum wavelength (275 nm). E is calculated by Eq. 1, where C_i and C_e represent the initial and final concentrations of ENR in terms of mg/L.

$$E = \frac{c_i - c_e}{c_i} \times 100\% \quad (1)$$

Please cite this article as: S. Shokrolahi, M. Farhadian, N. Davari, Degradation of Enrofloxacin antibiotic in contaminated water by ZnO/Fe_2O_3/Zeolite nanophotocatalyst, Journal of Applied Research in Water and Wastewater, 6 (2), 2019, 150-155.

3. Results and discussion

3.1. Nanophotocatalyst characterizations

3.1.1. XRD analysis

XRD results for clinoptilolite as well as ZnO/Fe_2O_3/Zeolite nanophotocatalyst are illustrated in Fig. 2. Zeolite have main peaks at 2θ values of 22.34° and 22.46°, corresponding to the reference peaks (Korkuna et al. 2006). Considering the different structures of zeolite extracted from diverse sources, there are some differences in their XRD patterns. ZnO/Fe_2O_3/Zeolite peaks can be observed at 2θ values of 31.82° and 36.19°, which correspond to the reference peaks (Hernández et al. 2007). The common peaks in the synthesized nanophotocatalyst and zeolite indicate that the position of the main zeolite peaks remains almost constant, suggesting the structure of zeolite as the support of the nanophotocatalyst. Since the iron content is less than 5 wt. %, the peaks associated with Fe^{3+} cannot be detected by XRD analysis (Hernández et al. 2007; Wang et al. 2011).

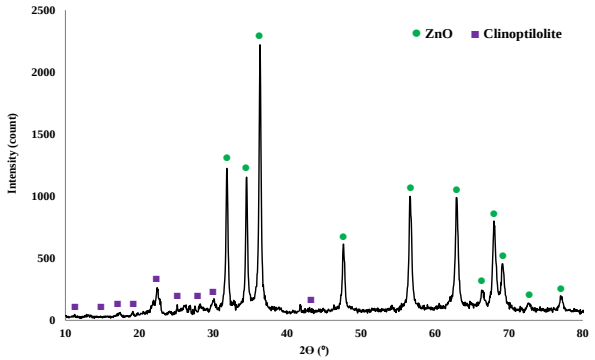

Fig. 2. XRD analysis of zeolite and ZnO/Fe_2O_3/Zeolite nanophotocatalyst.

3.1.2. XRF analysis

XRF analyses of ZnO/Fe_2O_3/Zeolite nanophotocatalyst and zeolite are illustrated in Table 3. The values of ZnO and Fe_2O_3 in the synthesized nanophotocatalyst are 55 and 3 wt. % in turn. In addition, the pre-calculated value of Fe^{3+}/ZnO (0.06) is successfully obtained in ZnO/Fe_2O_3/Zeolite nanophotocatalyst. The value of Si/Al in zeolite is equal to 6.11, suggesting thermal stability of zeolite (Cruciani. 2006).

Table 3. XRF analysis of zeolite and ZnO/Fe_2O_3/Zeolite nanophotocatalyst.

Compound	Zeolite concentration, wt. %	ZnO/Fe_2O_3/Zeolite concentration, wt. %
ZnO	-	55.70
SiO_2	79.73	30.55
Al_2O_3	11.52	4.72
CaO	1.95	0.83
Na_2O	1.93	-
K_2O	1.86	0.73
Fe_2O_3	1.41	3.44
MgO	1.06	0.46
TiO_2	0.19	0.08
SO_3	0.18	0.09
SrO	0.13	0.06
CuO	0.04	-
Cl	-	3.34
Total	100	100

3.1.3. FT-IR analysis

FT-IR spectra for ZnO/Fe_2O_3/Zeolite nanophotocatalyst and zeolite can be seen in Fig. 3. The peaks related to zeolite are also repeated in ZnO/Fe_2O_3/Zeolite nanophotocatalyst. In the synthesized nanophotocatalyst spectrum, additional peaks are observed at wave numbers of around 610, 460, and 3500 cm^{-1}, which are related to the functional group of Zn-O for ZnO nanoparticles, stretching vibration of Fe-O functional group of iron oxide nanoparticles, and superficial O-H hydroxyl group of zinc oxide and iron oxide particles, respectively (Hernández et al. 2007).

3.1.4. EDX and FE-SEM analysis

FE-SEM image and EDX spectrum for ZnO/Fe_2O_3/Zeolite nanophotocatalyst and zeolite with the scale of 375 nm are presented in Fig. 4. FE-SEM image in Fig. 4a indicates the smooth surface of zeolite, and Fig. 4b shows the surface of the synthesized nanophotocatalyst, where presence of deposited nanoparticles (ZnO/Fe_2O_3) is obvious. Based on Fig. 4b, the approximate size of the photocatalyst is around 48 nm. Moreover, the results of EDX spectrum confirm loading of Al and Si on zeolite (Fig. 4a) as well as loading of Zn and Fe on ZnO/Fe_2O_3/Zeolite photocatalyst (Fig. 4b).

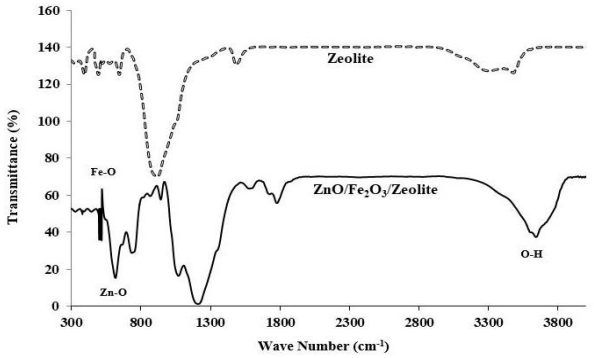

Fig. 3. FT-IR spectrum of zeolite and ZnO/Fe_2O_3/Zeolite nanophotocatalyst.

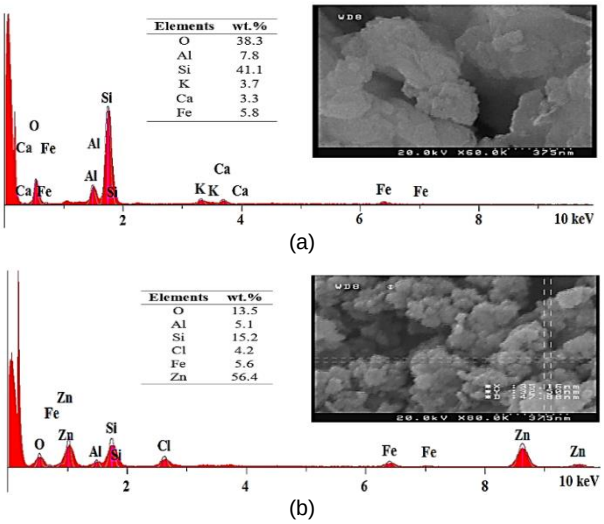

Fig. 4. EDX spectrum and FE-SEM image of (a) zeolite and (b) ZnO/Fe_2O_3/Zeolite nanophotocatalyst.

The diameter of the synthesized nanophotocatalyst particles is measured by ImageJ 1.44 p software, with Fig. 5 demonstrating particles size distribution. The particle size distribution ranges between 1 and 100 nm, and the synthesized nanophotocatalyst has around 30% particles with a diameter below 20 nm.

3.1.5. BET analysis

BET results of ZnO/Fe_2O_3/Zeolite nanophotocatalyst and zeolite are demonstrated in Table 4. The specific surface areas (m^2/g) for zeolite and the synthesized nanophotocatalyst are 370.45 and 280.16, and the pore volumes (cm^3/g) are 0.57 and 0.35, respectively. As can be seen, zeolite has a larger specific surface area and pore volume because successful deposition of ZnO/Fe_2O_3 on the surface and inside pores of zeolite reduce its surface area and pore volume (Davari et al. 2017).

Table 4. BET analysis of zeolite and ZnO/Fe_2O_3/Zeolite nanophotocatalyst.

Compound	BET surface area, m^2/g	Pore volume, cm^3/g
Zeolite	370.45	0.57
ZnO/Fe_2O_3/Zeolite	280.16	0.35

Please cite this article as: S. Shokrolahi, M. Farhadian, N. Davari, Degradation of Enrofloxacin antibiotic in contaminated water by ZnO/Fe_2O_3/Zeolite nanophotocatalyst, Journal of Applied Research in Water and Wastewater, 6 (2), 2019, 150-155.

3.2. Results of the photocatalytic experiments for ENR degradation

In this study, some experiments are performed in the absence of UV light in order to determine ENR adsorption on ZnO/Fe_2O_3/Zeolite nanophotocatalyst. The adsorption efficiency at all pH values and after 24-48 h is about 3 %. Moreover, prior to the photocatalytic tests, ENR degradation in dark condition is investigated within 2 h, which indicates that the removal of ENR is negligible. Therefore, the adsorption capacity of the nanophotocatalyst for the ENR degradation is neglected. Table 5 presents the results obtained from the design of experiments through RSM and with factors, including ENR concentration, initial pH of the solution, and H_2O_2 concentration across three levels for ENR degradation with ZnO/Fe_2O_3/Zeolite nanophotocatalyst. The analysis of the results and evaluation of the optimal conditions on the ENR degradation are determined by Design Expert version 8.0.1 software.

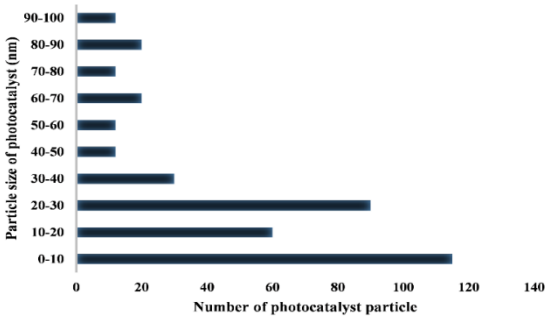

Fig. 5. Particles size distribution of ZnO/Fe_2O_3/Zeolite nanophotocatalyst.

Table 5. RSM results for the photocatalytic degradation of ENR.

Run number	A: Enrofloxacin concentration, mg/L	B: pH	C: H_2O_2 concentration, mg/L	E: Enrofloxacin degradation efficiency, %
1	300 ± 0.4	9 ± 0.01	50 ± 0.15	86.5 ± 0.3
2	450 ± 0.5	9 ± 0.01	100 ± 0.2	92.3 ± 0.4
3	150 ± 0.2	5 ± 0.01	100 ± 0.2	72.6 ± 0.2
4	300 ± 0.4	5 ± 0.01	50 ± 0.15	84.3 ± 0.3
5	150 ± 0.2	7 ± 0.01	200 ± 0.5	73.2 ± 0.2
6	450 ± 0.5	7 ± 0.01	200 ± 0.5	90.5 ± 0.4
7	150 ± 0.2	7 ± 0.01	50 ± 0.15	71.6 ± 0.2
8	300 ± 0.4	5 ± 0.01	200 ± 0.5	85.2 ± 0.3
9	300 ± 0.4	9 ± 0.01	200 ± 0.5	87.6 ± 0.3
10	300 ± 0.4	7 ± 0.01	100 ± 0.2	86.4 ± 0.3
11	300 ± 0.4	7 ± 0.01	100 ± 0.2	87.5 ± 0.3
12	450 ± 0.5	7 ± 0.01	50 ± 0.15	90.6 ± 0.4
13	450 ± 0.5	5 ± 0.01	100 ± 0.2	89.8 ± 0.3
14	300 ± 0.4	7 ± 0.01	100 ± 0.2	86.5 ± 0.3
15	150 ± 0.2	9 ± 0.01	100 ± 0.2	74.1 ± 0.2

The statistical analysis of data was performed by ANOVA, whose results are shown in Table 6. Assessment and data analysis are performed based on *p*-value (as the index for significance of factors) and *F*-value (as the index for priority of factors influence). Based on RSM principles, the factors with *p*-value less than 0.05 are considered significant, i.e. there is 5% error probability to assume an insignificant factor as a significant one (confidence interval 95%). Based on *p*-values in Table 6, the statistical model, ENR concentration, pH, and H_2O_2 concentration are significant factors, and there is no interaction between the factors. Additionally, according to *F*-values in Table 6, the factors, including ENR concentration, pH, and H_2O_2 concentration have the maximum impact on the ENR degradation efficiency, respectively.

Table 6. ANOVA for the photocatalytic degradation of ENR.

Model terms	DF	SS	MS	F-value	P-value	Status
Model	9	704.39	78.27	283.86	0.0001	Significant
A	1	614.43	614.43	2228.46	0.0001	Significant
B	1	9.53	9.53	34.55	0.0020	Significant
C	1	1.82	1.82	6.62	0.0499	Significant
A×B	1	0.61	0.61	2.21	0.1976	Insignificant
A×C	1	0.31	0.31	1.12	0.3389	Insignificant
B×C	1	0.13	0.13	0.46	0.5290	Insignificant
A^2	1	0.15	0.15	0.55	0.5041	Insignificant
B^2	1	0.17	0.17	0.62	0.4654	Insignificant
C^2	1	0.51	0.51	1.73	0.2516	Insignificant
Lack of Fit	3	0.21	0.071	0.12	0.9397	Insignificant

3.2.1. Model for the photocatalytic degradation of ENR

In this study, the second-order statistical model presented by Design Expert for the photocatalytic degradation of ENR is shown in Eq. 2, where A, B, C, and E represent ENR concentration, pH, H_2O_2 concentration, and the ENR degradation efficiency.

$$E = 86.67 + 8.76A + 1.09B + 0.48C \quad (2)$$

To indicate a good correspondence between the experimental data and the predicted responses, R^2 criterion is used, whose value range is between 0 and 1. R^2 value is 0.99, suggesting a suitable correspondence between the experimental and predicted results. In addition, the value of modified R^2 is 0.98, indicating the model's accuracy of fitting. The mentioned results are shown in Fig. 6.

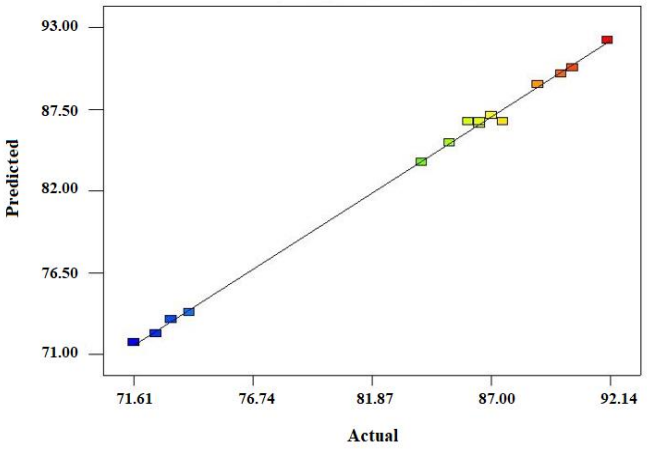

Fig. 6. Experimental results (□) and predicted results (／) for the photocatalytic degradation of ENR.

3.2.2. Effect of ENR concentration on the photocatalytic degradation of ENR

The effect of ENR concentration on the ENR degradation efficiency by ZnO/Fe_2O_3/Zeolite nanophotocatalyst is shown in Fig. 7. The nanophotocatalyst concentration, irradiation time, and pH are considered as 0.5 g/l, 120 min, and 7, respectively. According to the results, with an increase in ENR concentration from 150 to 450 mg/l at a constant H_2O_2 concentration, the degradation efficiency increases from around 75 to 91 %. The assumed reason is that when ENR concentration rises, more ENR molecules are adsorbed on the surface of the nanophotocatalyst, resulting in the increase in the ENR degradation efficiency up to the optimal nanophotocatalyst capacity (Esmaili et al. 2017).

Please cite this article as: S. Shokrolahi, M. Farhadian, N. Davari, Degradation of Enrofloxacin antibiotic in contaminated water by ZnO/Fe_2O_3/Zeolite nanophotocatalyst, Journal of Applied Research in Water and Wastewater, 6 (2), 2019, 150-155.

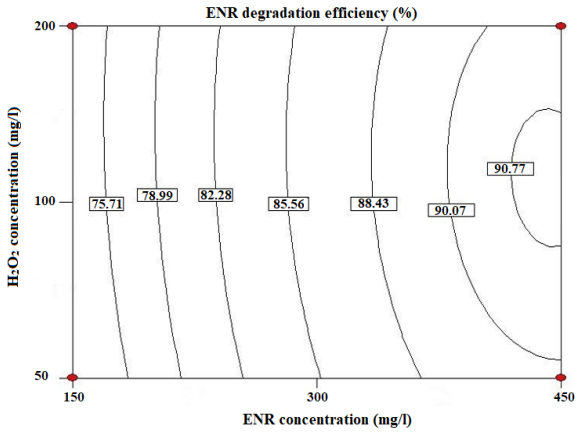

Fig. 7. Counter plot of ENR degradation efficiency as ENR concentration and H_2O_2 concentration.

3.2.3. Effect of H_2O_2 concentration on the photocatalytic degradation of ENR

The effect of H_2O_2 concentration and pH on the ENR degradation efficiency with ZnO/Fe_2O_3/Zeolite nanophotocatalyst is shown in Fig. 8. The nanophotocatalyst concentration, irradiation time, and ENR concentration are considered as 0.5 g/L, 120 min, and 300 mg/l, respectively. The results indicate that as H_2O_2 concentration grows from 50 to 200 mg/l at a constant pH, the degradation efficiency first increases and then decreases. This is due to the fact that with an increase in H_2O_2 concentration up to its optimal point, the degradation efficiency grows thanks to further produced $^{\bullet}OH$. Nevertheless, when H_2O_2 concentration increases at beyond its optimal point, the degradation efficiency drops because of $^{\bullet}OH_2$ formation which has less degradation efficiency (Taghvaei et al. 2017). Additionally, according to Fig. 8, with a rise in pH at a constant H_2O_2 concentration, the ENR degradation efficiency increases, obtaining the degradation efficiency of around 87% at alkaline pHs. At acidic pHs, ZnO loses its oxygen and turns into Zn^{2+}, dissolving in water and reducing its photocatalytic properties (Farzadkia et al. 2014). At alkaline pHs, ZnO has a greater ability in $^{\bullet}OH$ production (Davari et al. 2017), resulting in further ENR degradation. Therefore, the minimum degradation efficiency of ENR with ZnO/Fe_2O_3/Zeolite occurs at acidic pH, while the maximum degradation efficiency is achieved at alkaline pH.

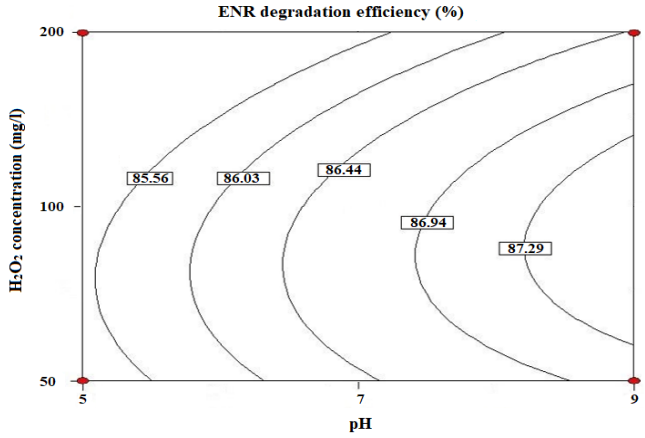

Fig. 8. Counter plot of ENR degradation efficiency as pH and H_2O_2 concentration.

3.2.4. Optimizing the photocatalytic degradation of ENR and recovery of ZnO/Fe_2O_3/Zeolite nanophotocatalyst

The experimental efficiency of ENR degradation is obtained as 97.4 %, while the degradation efficiency by the model is predicted as 98.5 % under optimal conditions (ENR concentration: 500 mg/L, pH=9, and H_2O_2 concentration: 90 mg/L). Therefore, the correspondence between the responses obtained from the experimental results and the statistical model suggests that the model presented by the software offers a good prediction of the experimental results for the ENR photocatalytic degradation. In a photocatalytic process, the stability of the photocatalyst activity and its recoverability are influential factors in the assessment of the photocatalyst performance. In this study, the stability of the synthesized ZnO/Fe_2O_3/Zeolite is examined under optimal conditions for the ENR degradation. After five replications of the experiment at optimal conditions (ENR concentration: 500 mg/l, pH=9, and H_2O_2 concentration: 90 mg/L), the ENR degradation efficiency with the synthesized nanophotocatalyst remains 97.4 %, resulting in a good stability and recoverability for the nanophotocatalyst.

4. Conclusions

This study indicates that the synthesized ZnO/Fe_2O_3/Zeolite can be used as an efficient method for degrading ENR antibiotic in pharmaceutical wastewater and water resources. The obtained results indicate that when ENR concentration and pH rise, the ENR degradation efficiency increases, while with an increase in H_2O_2 concentration, the degradation efficiency first increases and then decreases. The ENR degradation efficiency is achieved as 97.4%, and the synthesized nanophotocatalyst is still recoverable after five repetitions of the experiment under optimal conditions, including 500 mg/l ENR, pH=9, and 90 mg/l H_2O_2.

Nomenclature

ANOVA	Analysis of variance
AOPs	Advanced oxidation processes
BET	Brunauer emmett teller
DF	Degrees of freedom
EDX	Energy dispersive x-ray
ENR	Enrofloxacin antibiotic
FE-SEM	Field emission scanning electron microscope
FQ	Fluoroquinolone antibiotic
FT-IR	Fourier transform infrared
MS	Mean square
RSM	Response surface methodology
SS	Sum of squares
XRD	X-ray diffraction
XRF	X-ray fluorescence

Acknowledgement

This paper has been executed by cooperation and support of environmental research institute of University of Isfahan. The authors highly appreciate this cooperation and support.

References

Alexandrino D.A.M., Mucha A.P., Almeida C.M.R., Gao W., Jia Z., Carvalho M.F., Biodegradation of the veterinary antibiotics enrofloxacin and ceftiofur and associated microbial community dynamics, Science of The Total Environment 581-582 (2017) 359-368.

Amornpitoksuk P., Suwanboon S., Randorn C., Photocatalytic activities of silver compound modified activated carbon@ZnO: Novel ternary composite visible light-driven photocatalysts, Materials Science in Semiconductor Processing 84 (2018) 50-57.

Anirudhan T.S., Shainy F., Christa J., Synthesis and characterization of polyacrylic acid-grafted-carboxylic graphene/titanium nanotube composite for the effective removal of enrofloxacin from aqueous solutions: Adsorption and photocatalytic degradation studies, Journal of Hazardous Materials 324 (2017) 117-130.

Arimi A., Farhadian M., Solaymani Nazar A.R., Homayoonfal M., Assessment of operating parameters for photocatalytic degradation of a textile dye by Fe_2O_3/TiO_2/clinoptilolite nanocatalyst using Taguchi experimental design, Research on Chemical Intermediates 42 (2016) 4021-4040.

Chen Z., Chen X., Di J., Liu Y., Yin S., Xia J., Li H., Graphene-like boron nitride modified bismuth phosphate materials for boosting photocatalytic degradation of enrofloxacin, Journal of Colloid and Interface Science 492 (2017) 51-60.

Cruciani G., Zeolites upon heating: Factors governing their thermal stability and structural changes, Journal of Physics and Chemistry of Solids 67 (2006) 1973-1994.

Please cite this article as: S. Shokrolahi, M. Farhadian, N. Davari, Degradation of Enrofloxacin antibiotic in contaminated water by ZnO/Fe_2O_3/Zeolite nanophotocatalyst, Journal of Applied Research in Water and Wastewater, 6 (2), 2019, 150-155.

Davari N., Farhadian M., Solaymani Nazar A.R., Homayoonfal M., Degradation of diphenhydramine by the photocatalysts of ZnO/Fe_2O_3 and TiO_2/Fe_2O_3 based on clinoptilolite: Structural and operational comparison, Journal of Environmental Chemical Engineering 5 (2017) 5707-5720.

Davari N., Farhadian M., Solaymani Nazar A.R., Synthesis and characterization of Fe_2O_3 doped ZnO supported on clinoptilolite for photocatalytic degradation of metronidazole, Environmental Technology (2019) 1-13.

Deng J., Ya C., Ge Y., Cheng Y., Chen Y., Xu M., Wang H., Activation of peroxymonosulfate by metal (Fe, Mn, Cu and Ni) doping ordered mesoporous Co_3O_4 for the degradation of enrofloxacin, RSC Advances 8 (2018) 2338-2349.

Dolar D., Kosutic K., Perisa M., Babic S., Photolysis of enrofloxacin and removal of its photodegradation products from water by reverse osmosis and nanofiltration membranes, Separation and Purification Technology 115 (2013) 1-8.

Esmaili Z., Cheshmberah F., Solaymani Nazar A.R., Farhadian M., Treatment of florfenicol of synthetic trout fish farm wastewater through nanofiltration and photocatalyst oxidation, Environmental Technology 38 (2017) 2040-2047.

Farzadkia M., Rahmani K., Gholami M., Esrafili A., Rahmani A., Rahmani H., Investigation of photocatalytic degradation of clindamycin antibiotic by using nano-ZnO catalysts, Korean Journal of Chemical Engineering 31 (2014) 2014-2019.

Fink L., Dror I., Berkowitz B., Enrofloxacin oxidative degradation facilitated by metal oxide nanoparticles, Chemosphere 86 (2012) 144-149.

Guo H., Ke T., Gao N., Liu Y., Cheng X., Enhanced degradation of aqueous norfloxacin and enrofloxacin by UV-activated persulfate: Kinetics, pathways and deactivation, Chemical Engineering Journal 316 (2017) 471-480.

Hernandez A., Maya L., Sanchez-mora E., Sanchez E.M., Sol-gel synthesis, characterization and photocatalytic activity of mixed oxide $ZnO\text{-}Fe_2O_3$, Journal of Sol-Gel Science and Technology 42 (2007) 71-78.

Korkuna O., Leboda R., Skubiszewska-zieba J., Vrublevska T., Gunko V.M., Ryczkowski J., Structural and physicochemical properties of natural zeolites: clinoptilolite and mordenite, Microporous and Mesoporous Materials 87 (2006) 243-254.

Lu Z., Chen F., He M., Song M., Ma Z., Shi W., Yan Y., Lan J., Li F., Xiao P., Microwave synthesis of a novel magnetic imprinted TiO_2 photocatalyst with excellent transparency for selective photodegradation of enrofloxacin hydrochloride residues solution, Chemical Engineering Journal 249 (2014) 15-26.

Navanunez M.Y., Martinez-de La Cruz A., Nitric oxide removal by action of ZnO photocatalyst hydrothermally synthesized in presence of EDTA, Materials Science in Semiconductor Processing 81 (2018) 94-101.

Peng G., Li T., Ai B., Yang S., Fu J., He Q., Yu G., Deng S., Highly efficient removal of enrofloxacin by magnetic montmorillonite via adsorption and persulfate oxidation, Chemical Engineering Journal 360 (2019) 1119-1127.

Qiu W., Zheng M., Sun J., Tian Y., Fang M., Zheng Y., Zhang T., Zheng C., Photolysis of enrofloxacin, pefloxacin and sulfaquinoxaline in aqueous solution by UV/H_2O_2, UV/Fe(II), and UV/H_2O_2/Fe(II) and the toxicity of the final reaction solutions on zebrafish embryos, Science of The Total Environment 651 (2019) 1457-1468.

Siwinska-stefanska K., Fluder M., Tylus W., Jesionowski T., Investigation of amino-grafted TiO_2/reduced graphene oxide hybrids as a novel photocatalyst used for decomposition of selected organic dyes, Journal of Environmental Management 212 (2018) 395-404.

Sturini M., Speltini A., Maraschi F., Rivagli E., Pretali L., Malavasi L., Profumo A., Fasani E., Albini A., Sunlight photodegradation of marbofloxacin and enrofloxacin adsorbed on clay minerals, Journal of Photochemistry and Photobiology A: Chemistry 299 (2015) 103-109.

Su Y., Chen P., Wang F., Zhang Q., Chen T., Wang Y., Yao K., Lv W., Liu G., Decoration of $TiO_2/g\text{-}C_3N_4$ Z-scheme by carbon dots as a novel photocatalyst with improved visible-light photocatalytic performance for the degradation of enrofloxacin, RSC Advances 7 (2017) 34096-34103.

Taghvaei H., Farhadian M., Davari N., Maazi S., Preparation, characterization and photocatalytic degradation of methylene blue by Fe^{3+} doped TiO_2 supported on natural zeolite using response surface methodology, Advances in Environmental Technology 3 (2017) 205-216.

Wang C., Shi H., Li Y., Synthesis and characteristics of natural zeolite supported $Fe^{3+}\text{-}TiO_2$ photocatalysts, Applied Surface Science 257 (2011) 6873-6877.

Wang C., Yin L., Xu Z., Niu J., Hou L.A., Electrochemical degradation of enrofloxacin by lead dioxide anode: Kinetics, mechanism and toxicity evaluation, Chemical Engineering Journal 326 (2017) 911-920.

Wen X.J., Niu C.G., Zhang L., Liang C., Zeng G.M., A novel Ag_2O/CeO_2 heterojunction photocatalysts for photocatalytic degradation of enrofloxacin: possible degradation pathways, mineralization activity and an in depth mechanism insight, Applied Catalysis B: Environmental 221 (2018) 701-714.

Xiong J.Q., Kurade M.B., Jeon B.H., Ecotoxicological effects of enrofloxacin and its removal by monoculture of microalgal species and their consortium, Environmental Pollution 226 (2017) 486-493.

Yi X., Lin C., Ong E.J.L., Wang M., Zhou Z., Occurrence and distribution of trace levels of antibiotics in surface waters and soils driven by non-point source pollution and anthropogenic pressure, Chemosphere 216 (2019) 213-223.

Yu Y., Yan L., Cheng J., Jing C., Mechanistic insights into TiO_2 thickness in $Fe_3O_4@TiO_2$-GO composites for enrofloxacin photodegradation, Chemical Engineering Journal 325 (2017) 647-654.

Zhu X., Liang X., Wang P., Dai Y., Huang B., Porous Ag-ZnO microspheres as efficient photocatalyst for methane and ethylene oxidation: Insight into the role of Ag particles, Applied Surface Science 456 (2018) 493-500.

Please cite this article as: S. Shokrolahi, M. Farhadian, N. Davari, Degradation of Enrofloxacin antibiotic in contaminated water by ZnO/Fe_2O_3/Zeolite nanophotocatalyst, Journal of Applied Research in Water and Wastewater, 6 (2), 2019, 150-155.